MEMOIRS OF THE FACULTY OF ENGINEERING
FUKUI UNIVERSITY
VOL.28 No.1 1980

Various Types of Magnetisms in SnTe Crystals Doped with 3d Transition Metals

Masasi INOUE*, Hiroto OSHIMA*, Motoji MORISAKI*, Hisao YAGI*, Hoong Kun FUN** and Toshiaki TATSUKAWA***

(Received Jan. 31, 1980)

Magnetization, ESR, and transport measurements have been carried out to study the various types of magnetisms in the degenerate magnetic semiconductor systems $Sn_{1-x}(Me)_xTe$ with different 3d transition metals Me=Cr, Fe, Co, and Ni. $Sn_{1-x}Cr_xTe$ exhibits a paramagnetic-ferromagnetic transition at the Curie temperatures T_c=150-300 K depending on the Cr concentration, as determined by magnetic and ESR measurements; in particular, the ESR field H_o and the linewidth ΔH both show a critical-divergence-like anomaly near T_c. Moreover, the temperature dependence of the resistivity of $Sn_{1-x}Cr_xTe$ shows other magnetic transitions, which are tentatively attributed to the formation of a preferred direction for the magnetic spins through the change in the crystalline symmetry associated with a ferroelectric phase transition of the host SnTe matrix. The other systems (except probably for $Sn_{1-x}Ni_xTe$) also exhibit magnetic transitions at liquid helium temperatures as found by transport measurements. This preliminary study (on all unoriented crystals) has shown that $Sn_{1-x}(Me)_xTe$ is an interesting system and should demand much more detailed further studies.

* Dept. of Applied Physics.
** On sabbatical leave from School of Physics, Universiti Sains Malaysia.
*** Exp. Lab. for Low Temp. Phys.

1. INTRODUCTION

Over the past several years it has been well established that mixed crystal of the narrow-gap semiconductor SnTe and the antiferromagnetic material MnTe, $Sn_{1-x}Mn_xTe$, becomes a degenerate magnetic semiconductor exhibiting a weak ferromagnetism at low temperatures through long-range indirect exchange interactions of the Mn impurity spins via conduction carriers.[1,2] Recently we have pointed out that in this alloy system there is a possibility of paramagnetic-antiferromagnetic-ferromagnetic transitions.[3] However, its experimental verification and the origins of these weak magnetic orderings are not clear at present and these are still under investigation.

In order to understand the properties of the degenerate magnetic semiconductor further, we have attempted here to make solid solutions of SnTe with other 3d transition elements such as Cr, Fe, Co, and Ni [thereafter referred to as transition metals denoted by (Me)]; we may be able to express this alloy system in the form $[SnTe]_{1-x}[(Me)Te]_x$ or $Sn_{1-x}(Me)_xTe$. To see any possibility of incorporating these Me elements into the host SnTe crystal, their ionic radii are compared with those of the host crystal, as compiled in Table I,[4] where the ions are assumed to be divalent or trivalent. It is observed that these Me ions are all smaller in size

Table I. Ionic radii of 3d transition metals.[4]

$3d^n$	$3d^3$	$3d^4$		$3d^5$		$3d^6$	$3d^7$	$3d^8$
Ions	Cr^{3+}	Cr^{2+}	Mn^{3+}	Mn^{2+}	Fe^{3+}	Fe^{2+}	Co^{2+}	Ni^{2+}
r (Å)	0.63	0.89	0.66	0.80	0.64	0.74	0.72	0.69

Hosts: Sn^{2+}; 0.93 Å, Te^{2-}; 2.11 Å.

than the host cations which the magnetic ions replace. In this paper we report the preliminary data on magnetic, transport, and spin resonance measurements of the alloy system of $Sn_{1-x}(Me)_xTe$, with emphasis on $Sn_{1-x}Cr_xTe$ (Me=Cr).

2. EXPERIMENTAL

Instead of mixing the three starting elements (Sn, Te, and Me) directly, the Me tellurides (Me)Te were first synthesized at 1100°C in a sealed quartz ampule for a few hours. Next the mixed crystals,

$Sn_{1-x}(Me)_xTe$, were grown by the Bridgman method at a lowering rate of 2 mm/hr. The grown ingot was cut by a spark cutting machine into a rectangular shape (typically 1 x 1 x 8 mm^3) for electrical measurements or a disk shape (4-5 mm thick and 8 mm diameter) for magnetization measurements. For spin resonace experiments the crystals were usually crushed into powder to decrease the skin effect as was done for SnTe-MnTe.[5] However, we found lately that even single crystals can be used for spin resonance studies when the crystal surface becomes smooth after mechanical polishing (final lapping powder; 0.3 μ alumina) and chemical etching. Some of the as-grown crystals were annealed at 600°C under Zn vapor to reduce the carrier concentration and to dope the magnetic impurities effectively, as often employed for SnTe-MnTe.

The experimental data shown here are mostly concerned with the magnetic measurements in the temperature range 77 K-500°C using a vibrating sample magnetometer operated at 80 Hz (VSM-3 type, Toei Ind. Co). The absolute value of magnetization was calibrated by a standard sample of nickel (the saturation magnetization at 20°C σ_s=54.39 emu/g) and the linearity of the apparatus (Hall probe for a magnetic field) was checked by Gd_2O_3 powder using its σ-H relation. The electrical properties were measured by a potentiometric method and a conventional X-band ESR spectrometer was employed for spin resonance experiments.

3. RESULTS AND DISCUSSIONS

3.1 Magnetic Measurements

A. (Me)Te

First we have examined the properties of the polycrystalline samples of the synthesized Me tellurides (Me)Te. Figure 1 shows their magnetization curves up to 5 kOe at room temperature. One should give attention to the magnitude of the magnetization per gram σ (emu/g) of each compound, as indicated in the figure caption. Excepting for NiTe, these tellurides show the typical hysteresis curves characteristic of ferromagnets; the ferromagnetism decreases in the order of CrTe, CoTe, and FeTe. Only NiTe is paramagnetic.

The residual magnetization at about 30 Oe for CrTe, CoTe and FeTe and the magnetization at 10 kOe for NiTe are shown in Fig. 2 as a function of temperature. From these σ-T curves, one can determine the ferromagnetic Curie temperature T_c. The value T_c for CrTe

was found to be 341 K, in agreement with the reported values of T_c= 340∿350 K.[6,7] The other samples show almost temperature-independent behaviors up to 500°C.

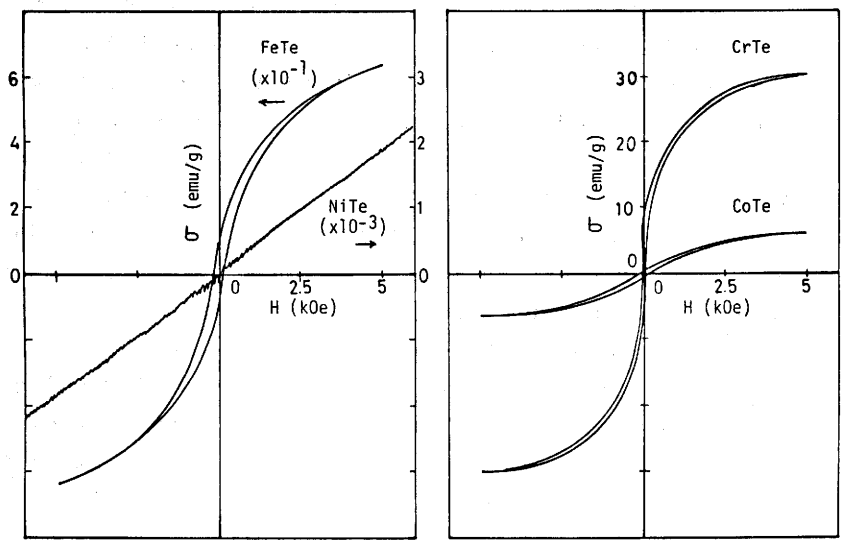

Fig. 1. Magnetization curves of various 3d transition metal tellurides (Me)Te at room temperature. The value of σ (emu/g) for FeTe or NiTe is to be multiplied to the left- or right-hand scale by the factor indicated below each compound.

In the present work we are not interested in the detailed properties of the (Me)Te themselves; various magnetic properties of these Me chalcogenides with NiAs type structure have been investigated by other workers.[6] Our main concern are the $Sn_{1-x}(Me)_xTe$.

B. $Sn_{1-x}(Me)_xTe$

First we have carried out the magnetization measurements of the undoped SnTe host crystals. Table II summarizes the observed diamagnetism at two fixed temperatures for the as-grown and the annealed crystals. The temperature dependence of the diamagnetic susceptibility was found to be rather gradual between 300 K and 77 K.

Figure 3 shows the magnetization curves at 77 K for the various as-grown mixed crystals $Sn_{1-x}(Me)_xTe$ (Me=Cr, Mn, Fe, Co and Ni), all with x=1 at.%. It is interesting to note that there exist different types of magnetisms among the alloy systems. The Cr- and Fe- doped crystals show a ferromagnetic hysteresis loop, whereas the Co- and Ni-doped ones are diamagnetic. Only Mn-doped crystals are paramagnetic.

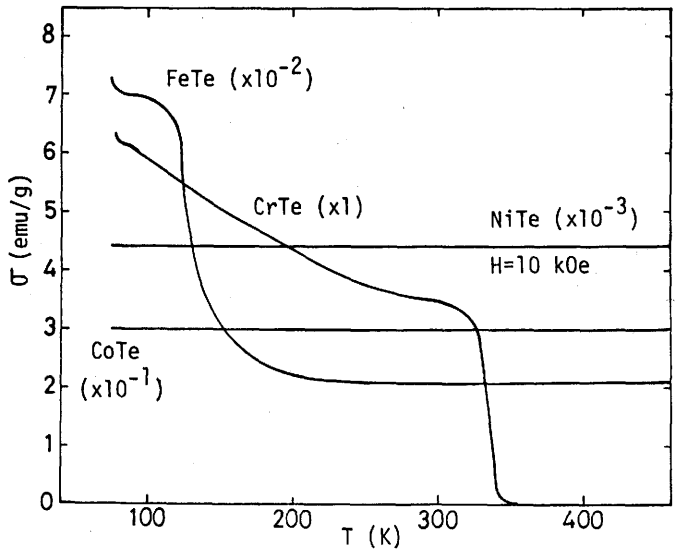

Fig. 2. Residual magnetization at about 30 Oe for CrTe, CoTe, and FeTe and the magnetization at 10 kOe for NiTe plotted against temperature. The value of σ for each sample is to be multiplied by the factor indicated.

Table II. Diamagnetic susceptibility χ_g (x 10^{-7} emu/g) of as-grown and annealed SnTe at 300 K and 77 K.

	300 K	77 K
as-grown	-4.0	-4.4
annealed	-3.6	-3.9

The temperature dependence of the magnetization of these crystals is illustrated in Fig. 4. Only the curve for the Mn-doped crystal follows a paramagnetic Curie-Weiss law, as already reported elsewhere .[8] The Cr-doped crystal is ferromagnetic at low temperatures and becomes diamagnetic at high temperatures. The Fe-doped crystal shows almost temperature-independent ferromagnetism up to 500°C; usually one cannot raise the temperature above 500°C because these crystals will sublimate. The temperature variation of the diamagnetic susceptibilities of the Co- and Ni-doped samples is quite similar to that of the host SnTe crystal, their magnitudes being of the same order.

For further understanding of these different types of magnetisms, extensive studies will be required, such as the variations of their properties with magnetic impurity concentrations. So far we have

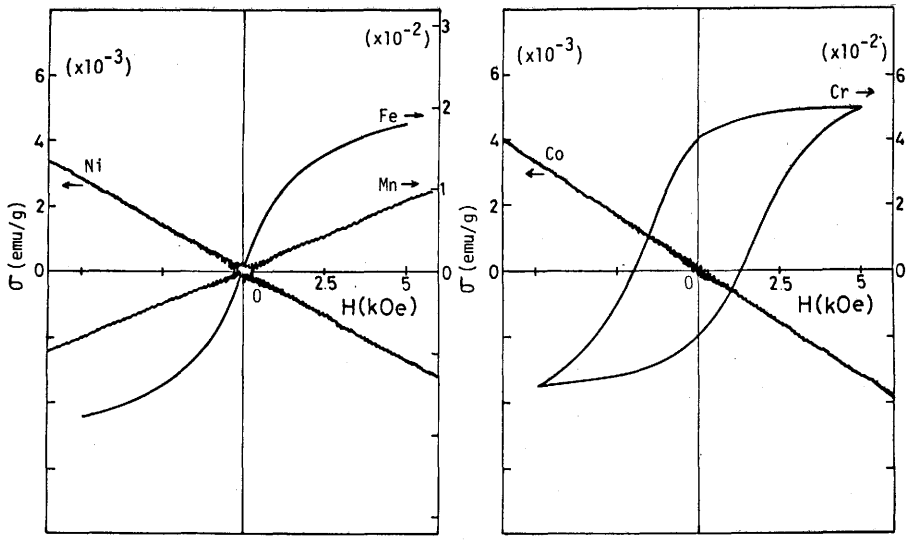

Fig. 3. Magnetization curves at 77 K for various as-grown $Sn_{1-x}(Me)_xTe$ crystals with Me=Cr, Mn, Fe, Co, Ni (x=1 at.%).

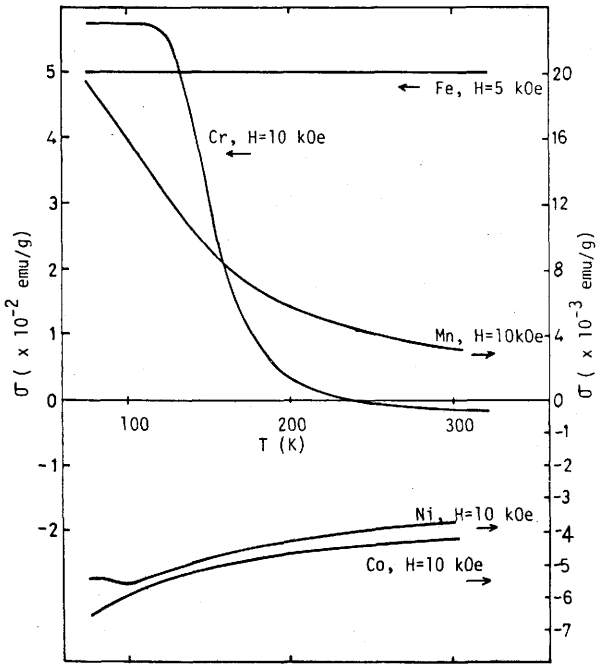

Fig.4. Temperature dependence of the magnetization for the as-grown $Sn_{1-x}(Me)_xTe$ crystals with Me=Cr, Mn, Fe, Co, Ni (x=1 at.%); the applied magnetic field is indicated for each sample.

investigated with much more details the Cr-doped crystals $Sn_{1-x}Cr_xTe$, which will be described below.

C. $Sn_{1-x}Cr_xTe$

The residual magnetizations at 30 Oe as a function of temperature are shown in Fig. 5 for the as-grown and annealed $Sn_{1-x}Cr_xTe$ crystals with different Cr concentrations. The ferromagnetic Curie temperatures obtained from these σ_r-T curves are seen to be strongly dependent on both the impurity concentration and the effect of heat treatment, as compiled in Fig. 6.

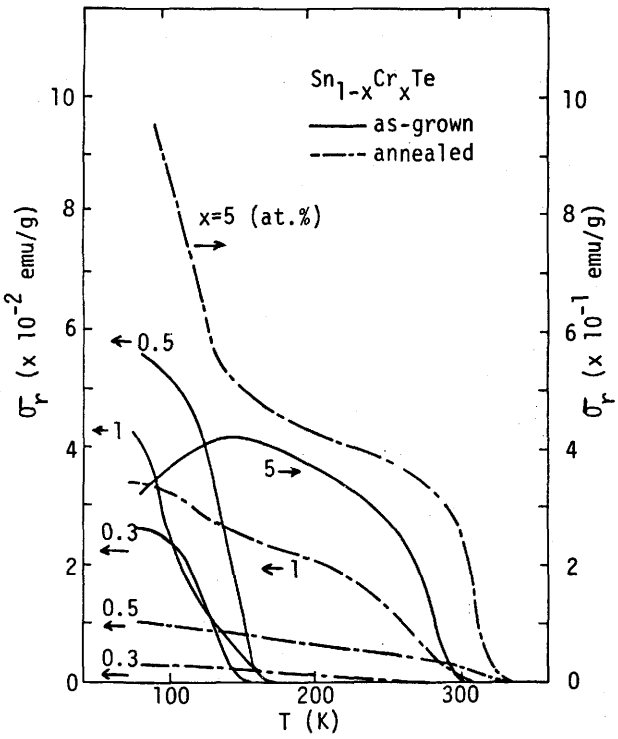

Fig. 5. Temperature dependence of the residual magnetization at about 30 Oe for the as-grown and annealed $Sn_{1-x}Cr_xTe$ with different x values.

It is to be noted that T_c for the annealed crystals is almost independent of x, while T_c for the as-grown crystals decreases with decreasing x.

Finally, Fig. 7 shows the three different magnetic properties of the as-grown $Sn_{1-x}Cr_xTe$ crystals, the magnetization at 5 kOe, σ,

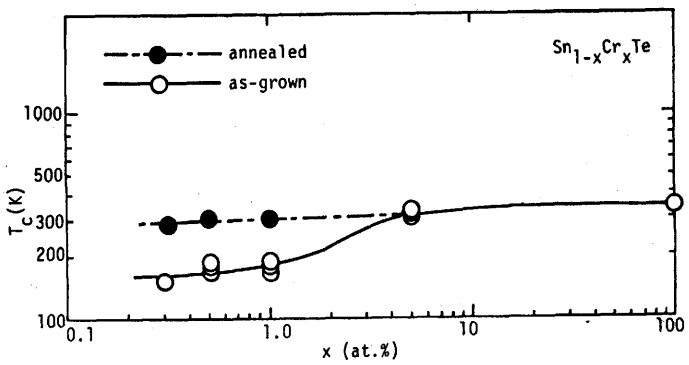

Fig. 6. The ferromagnetic Curie temperatures obtained from the σ_r-T curves for the as-grown and annealed $Sn_{1-x}Cr_xTe$ plotted against x.

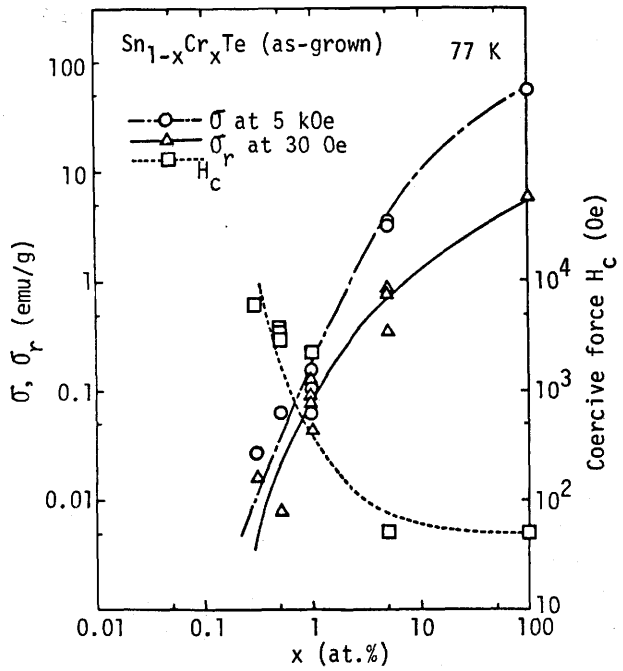

Fig. 7. The magnetization at 5 kOe, the residual magnetization at 30 Oe, and the coercive force at 77 K for the as-grown $Sn_{1-x}Cr_xTe$ plotted against x.

the residual magnetization at 30 Oe, σ_r, and the coercive force, H_c, at 77 K as a function of the Cr concentration. Similar behaviors were also found for the annealed $Sn_{1-x}Cr_xTe$ crystals. These values for the as-grown and annealed crystals are given in Table III. It is seen that these magnetic quantities depend strongly on the impurity concentration. The decreases in σ and σ_r with decreasing x become drastic for $x < 1$ at.%; the magnetization σ is likely seen to vanish at around a critical concentration x_c=0.2-0.3 at.%, though this critical value is not certain. In contrast, another quantity that characterizes the ferromagnetism in this alloy system, such as the Curie temperature T_c shown in Fig. 6, is not so drastic around x_c. Furthermore, from Table III we observe that the magnetic impurity distribution throughout a grown ingot is not homogeneous. Such an inhomogeneous distribution has also been found even in the Bridgman-grown $Sn_{1-x}Mn_xTe$ crystals studied thus far.

The material CrTe itself is ferromagnetic below T_c. Normally from the saturation magnetization $\sigma_s(0)$ at T=0, estimated from σ measurements at low temperatures, an effective magnetic moment μ_f per metal atom can be calculated using the equation $\mu_f=\sigma_s M/5585$,

Table III. Magnetization at 5 kOe σ, residual magnetization σ_r, and coercive force H_c at 77 K for as-grown and annealed $Sn_{1-x}Cr_xTe$.

	as-grown			annealed		
x (at.%)	σ (emu/g)	σ_r (emu/g)	H_c (Oe)	σ (emu/g)	σ_r (emu/g)	H_c (Oe)
100	53	5.5	50			
5	3.3	0.83	50	3.3	0.49	50
	3.1	0.74	50	1.9	0.97	100
	3.0	0.33	50			
1	0.061	0.042	2150	0.053	0.034	275
	0.17	0.14	1650	0.085	0.064	925
	0.083	0.069	5000			700
	0.079	0.050	1600			
0.5	0.062	0.056	3600	0.019	0.0098	450
	0.0086	0.0079	3350			
	0.062	0.053	2800			
0.3	0.027	0.026	4850	0.027	0.028	1200

in units of Bohr magnetons μ_B, where M is the molecular weight. Lotgering and Gorter[6] obtained μ_f=2.45 μ_B with σ_s=76.2 emu/g for CrTe. A rough estimation of our value for CrTe gives μ_f=1.8 μ_B with $\sigma_s \simeq$55 emu/g at 5 kOe, which is slightly less than theirs. For $Sn_{1-x}Cr_xTe$ with x=1 at.% and $\sigma_s \simeq$0.1 emu/g, we get roughly μ_f= $246.29\sigma_s/(5585 \times 0.01) \simeq 0.44$ μ_B, which is much smaller than the free atom's value. This small value of μ_f for the $Sn_{1-x}Cr_xTe$ (x=1 at.%) crystal indicates that the ferromagnetic ordering between the Cr ions is due to long-range (or indirect) exchange interactions via conduction carriers.

3.2 Electrical Measurements

As one of the spin dependent transport properties of the SnTe-MnTe system, we have measured an anomalous Hall effect,[2,9] which arises from the asymmetrical scatterings of conduction carriers and depends on the state of magnetization of the crystals. For this alloy system the anomalous Hall coefficient R_1 was found to depend quadratically on temperature and to vanish at some temperature, which is in agreement with a theoretical model based on the interaction between conduction electrons and localized magnetic electrons with a mixed spin-orbit interaction.

Similar measurements were carried out on the annealed crystals of $Sn_{1-x}(Me)_xTe$ all with x=1 at.%. The anomalous Hall coefficient R_1 and the corresponding electrical resistivity ρ of each sample (Me=Cr, Fe, Co, and Ni) as a function of temperature are shown in Figs. 8 and 9, respectively. The dotted lines shown in Fig. 8 are the temperatures (we denoted them by T_c in a previous paper[2]) at which the anomalous Hall effect vanishes and coincides with the ordinary Hall effect. These characteristic temperatures are indicated by the arrows in Fig. 9. No such anomalous behaviors of R_1 and ρ were observed in the as-grown $Sn_{1-x}(Me)_xTe$ crystals. The Ni-doped crystal does not show any anomalous behaviors, whereas other crystals doped with Cr, Fe, and Co exhibit similar variations to those of the Mn-doped crystal. We should note, however, that the magnetic transition temperatures of the Cr-, Fe-, and Co-doped crystals determined by the magnetization measurements are much higher ($T > 150$ K) than those shown in Fig. 9 ($T < 6$ K) found by the transport measurements. At present we cannot draw any definite conclusion of the magnetic states in these $Sn_{1-x}(Me)_xTe$

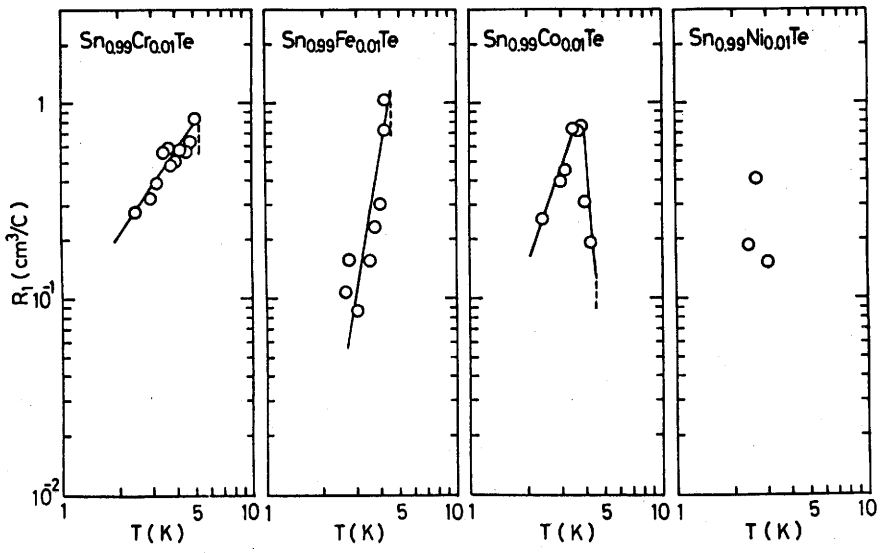

Fig. 8. Temperature dependence of the anomalous Hall coefficient R_1 for the annealed $Sn_{1-x}(Me)_xTe$ with Me=Cr, Fe, Co, Ni (x=1 at.%).

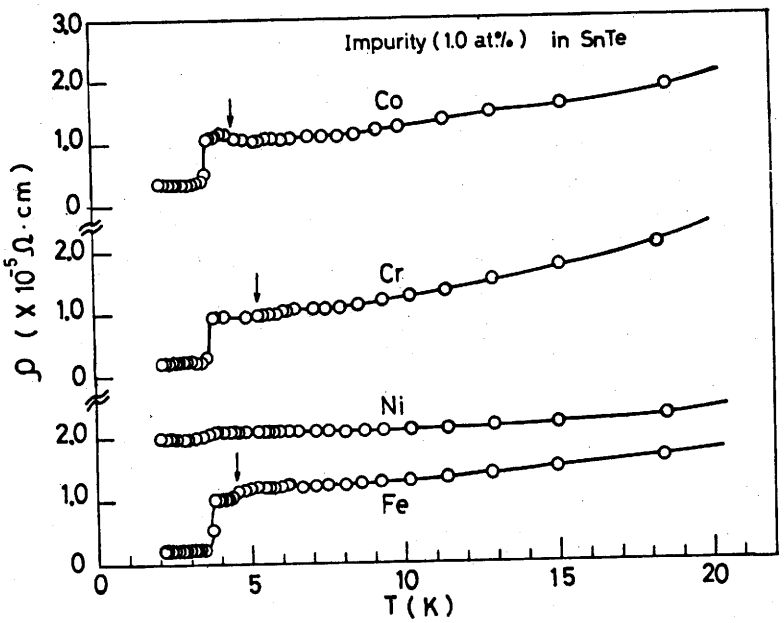

Fig. 9. Temperature dependence of resistivity for the annealed $Sn_{1-x}Cr_xTe$ with Me=Cr, Fe, Co, Ni (x=1 at.%). The arrows indicate the temperatures at which the anomalous Hall effect vanishes.

systems. A possible explanation may be that these systems undergo several stages of magnetic transitions (like metamagnetism) as the temperature is lowered. Detailed measurements of magnetization as well as specific heat will provide us with more confirmative information.

3.3 Spin Resonance Measurements

Electron spin resonance (ESR) is also a powerful technique for understanding the electronic states in various solids. So far we have carried through the ESR measurements on the SnTe-MnTe system and obtained valuable information.[8,10] The samples used were all annealed crystals and were crushed into powder to reduce the skin effect, which we believed is effective for the ESR experiments. The single crystals, whose surfaces were polished by lapping powder of #3000 mesh and etched by a solution of HNO_3 and NaOH, reduced the Q-dip of the ESR cavity appreciably. Thus powdered samples have been exclusively used in our own laboratory over the past several years. However, recently one of us (H.K.F.) has pointed out that this is not the case. Though our Bridgman-grown crystals, possessing several grain boundaries, are not complete and good single crystals, we have found that the single (but unoriented) crystals, after lapping the surfaces to a mirror-like finish (by using finer lapping powder of 0.3μ alumina and followed by chemical etching) produce good ESR signals with linewidths narrower when compared with those of the powdered samples. This effect was clearly seen in the present alloy systems of $Sn_{1-x}(Me)_xTe$, as shown below; a typical linewidth ΔH for Cr-doped SnTe at 300 K was 2000-3000 G in the case of powdered samples compared with $\Delta H \simeq 400$ G for a single crystal of a rectangular shape (typically 1x1x8 mm^3). The spin resonance data were taken by an X-band ESR spectrometer in the temperature range 150-360 K. As in $Sn_{1-x}Mn_xTe$, the as-grown $Sn_{1-x}(Me)_xTe$ crystals did not show any resonance signals; also no signals were observed in the annealed crystals doped with Fe, Co, and Ni (all 1 at.%). In what follows, we shall present the preliminary data on the ferromagnetic resonance of the Cr (1 at.%)-doped annealed crystal alone, which is found to be a ferromagnetic substance according to the magnetic measurements. Even though the experimental data shown below are only preliminary, they seem to be strongly indicative of ferromagnetic resonance (FMR) signals, which we would like to stress here. In the

Appendix, we summarize the characteristic features of FMR for ferromagnets[11-13] as well as antiferromagnetic resonance (AFMR) for antiferromagnets.[14-16]

Figure 10 depicts the temperature variation of the observed resonance signals at a microwave frequency of 9260 MHz for the annealed $Sn_{1-x}Cr_xTe$ (x=1 at.%) crystal, the crystal orientation being fixed with respect to the static magnetic field. We can see the marked shift of the resonance field H_o and the variation of the linewidth ΔH as the temperature is varied through the Curie temperature T_c.

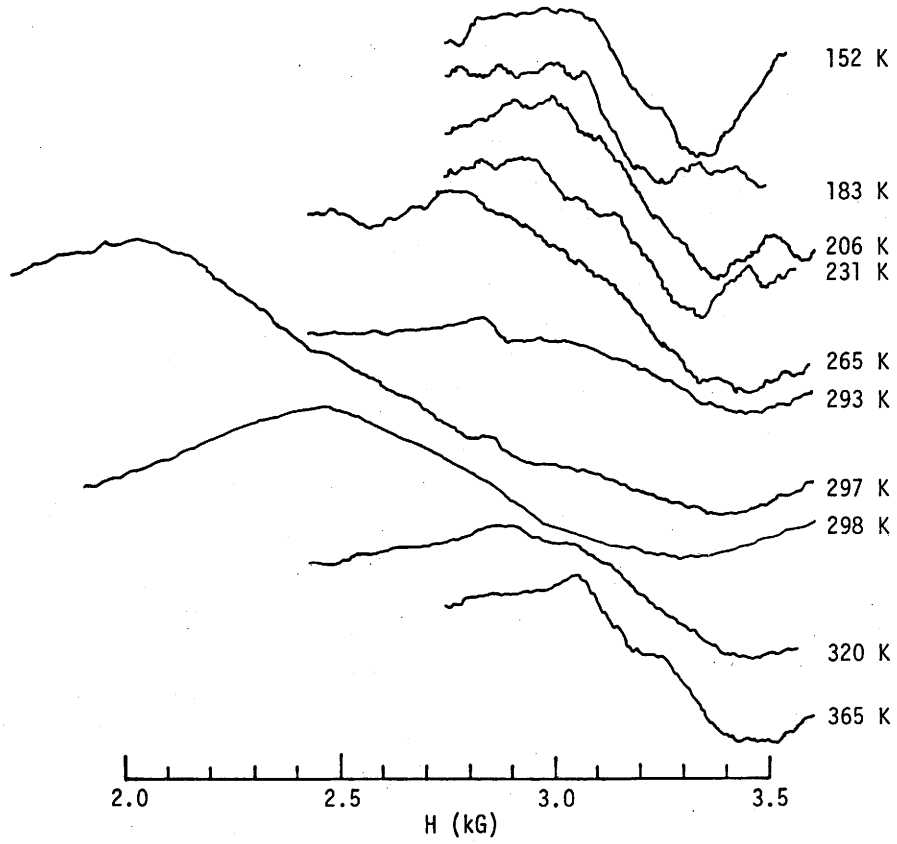

Fig. 10. Temperature variations of the resonance signals for the annealed $Sn_{1-x}Cr_xTe$ crystal with x=1 at.%, at a fixed crystal orientation with respect to the static magnetic field, measured at a microwave frequency of 9260 MHz. The scale shown indicates the applied magnetic field.

Figures 11 and 12 show these values plotted as a function of temperature. Near the ferromagnetic Curie temperature T_c=293 K,

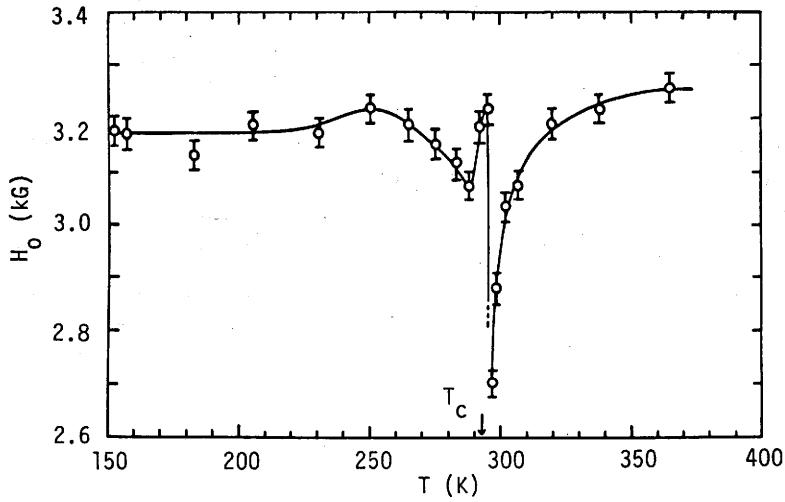

Fig. 11. Temperature variation of the resonance field H_o at a microwave frequency 9260 MHz for the annealed $Sn_{1-x}Cr_xTe$ crystal with x=1 at.%; T_c is the ferromagnetic Curie temperature determined from the magnetic measurements.

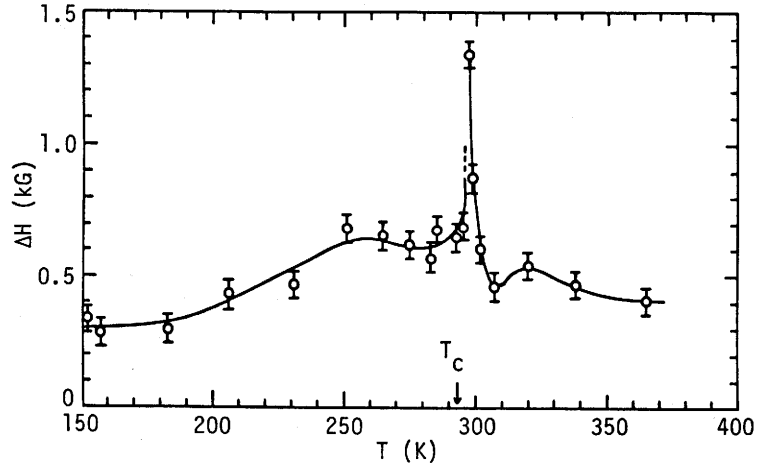

Fig. 12. Temperature variation of the linewidth ΔH for the annealed $Sn_{1-x}Cr_xTe$ crystal with x=1 at.%; T_c is the ferromagnetic Curie temperature determined from the magnetic measurements (see also Fig. 5).

both H_o and ΔH show an anomalous behavior like "critical divergence", the critical region being of the order of ΔT=10-20 K. In view of the characteristic features of FMR and AFMR described in the Appendix, the above preliminary data of the $Sn_{1-x}Cr_xTe$ crystal are strongly indicative of the presence of either or both types of resonance signals. Also it should be emphasized that the ferro- or antiferromagnetism in this system is quite weak and different from the representative bulk ferromagnets or antiferromagnets. In our case the magnetic impurities are dissolved in the host matrix with a strong background diamagnetic contribution and the magnetic interactions of long-range or exchange type are through conduction carriers. In this sense our system is very interesting. Thus it is expected that the magnetic transition near T_c is paramagnetic-ferromagnetic based on the magnetic and ESR measurements or, more in general, probably paramagnetic-antiferromagnetic-ferromagnetic based on the ESR measurements. However, in order to confirm these possibilities, we have to measure more precisely the temperature variation of the quantities such as H_o or ΔH near the transition temperatures. In addition, the samples to be used must be oriented crystals and have more symmetrical forms like cylindrical or spherical shapes to simplify the data analysis and get more reliable information.

4. CONCLUSIONS

Thus far we have found that the $Sn_{1-x}Cr_xTe$ crystal undergoes a paramagnetic-ferromagnetic transition at a well-defined Curie temperature of about 150-300 K depending on the Cr concentration; here the paramagnetic state of the Cr impurities is actually dominated by the bulk background diamagnetic contribution of the host SnTe crystal. This has been confirmed by the magnetization and ESR experiments. The other systems of $Sn_{1-x}(Me)_xTe$ (Me=Mn, Fe, Co, and Ni) also exhibit different types of magnetisms as found by the magnetization measurements. On the other hand, the transport measurements on the $Sn_{1-x}Cr_xTe$ crystals have shown the presence of other characteristic temperatures appearing in the liquid helium temperatures, which may also correspond to some other magnetic transitions. The other systems (excepting $Sn_{1-x}Ni_xTe$) also exhibit magnetic transitions at liquid helium temperatures as shown by transport measurements.

A possible explanation for these magnetic orderings at low temp-

eratures is tentatively considered as follows: It is well known that the host matrix of SnTe is a "near ferroelectric" material analogous to the perovskite ferroelectrics $SrTiO_3$ and $BaTiO_3$. These systems undergo a structural (ferroelectric) phase transition at a critical temperature. For SnTe this transition, associated with a softening of the TO phonons, occurs at around 80-100 K depending on the carrier concentrations.[10,17] Thus the crystal symmetry changes from a cubic to a rhombohedral structure, usually by an elongation along the <111> direction, resulting in the change of the crystalline environment around the magnetic impurities. As a result, this could induce a preferred direction for the magnetic spins to orientate along with and thus possibly produce extra antiferromagnetic or ferromagnetic orderings through indirect exchange interactions.

In view of all of these facts, our degenerate magnetic semiconductors are complicated systems showing a variety of magnetic ordering states, their origins being probably due to indirect exchange interactions between spins (of localized or itinerant nature) via conduction carriers. Full understanding of these mechanisms will require a variety of experiments over a wide range of temperatures, including specific heat measurements. Table IV summarizes the

Table IV. Summary of the different types of magnetisms in the Me chalcogenides (Me)Te and $Sn_{1-x}(Me)_xTe$ with x=1 at.% as determined by magnetic measurements, and the results of spin resonance at room temperature on $Sn_{1-x}(Me)_xTe$ with x=1 at.%.

Me	(Me)Te	$Sn_{1-x}(Me)_xTe$	Spin resonance
Cr	F	F	FMR
Mn	AF	P	EPR
Fe	F	F	No signal
Co	F	D	No signal
Ni	P	D	No signal

F: Ferromagnetic, AF: Antiferromagnetic, P: Paramagnetic,
D: Diamagnetic.
FMR: Ferromagnetic resonance is observable.
EPR: Electron paramagnetic resonance is observable.

present results on the Bridgman-grown $Sn_{1-x}(Me)_xTe$ crystals with repect to the different types of magnetisms as well as the spin resonance. We must note, however, that these are not conclusive.

ACKNOWLEDGMENTS

One of us (H.K.F.) is grateful to Japan Society for the Promotion of Science for financial support during his sabbatical stay at this Department. We also thank Professors A. Yanase (Tohoku Univ.), M. Date and K. Okuda (Osaka Univ.) for valuable discussions. Finally, thanks are due to Mr. S. Tanaka for ESR measurements, Mr. K. Tsubokawa and Mr. T. Saito for low temperature techniques.

REFERENCES

1) M. Inoue, M. Fukuoka and H. Yagi: J. Phys. Soc. Jpn. 47 (1979) 1836.
2) M. Inoue, M. Tanabe, H. Yagi and T. Tatsukawa: J. Phys. Soc. Jpn. 47 (1979) 1879.
3) H. K. Fun, M. Inoue and H. Yagi: Mem. Fac. Eng. Fukui Univ. 28, No. 1 (1980), this issue.
4) R. C. Wead ed.: CRC Handbook of Chemistry and Physics (Chemical Rubber, 1970) 51st ed.
5) M. Inoue, H. Yagi and Y. Kamino: J. Phys. Soc. Jpn. 34 (1973) 561.
6) F. K. Lotgering and E. W. Gorter: J. Phys. Chem. Solids 3 (1957) 238.
7) H. Haraldsen and A. Neuber: Z. Anorg. Chem. 234 (1937) 353.
8) M. Inoue, H. Yagi, T. Muratani and T. Tatsukawa: J. Phys. Soc. Jpn. 40 (1976) 458.
9) M. Inoue, K. Ishii and H. Yagi: J. Phys. Soc. Jpn. 43 (1977) 903.
10) K. Sugawara, C. Y. Huang, M. Inoue, H. Yagi and T. Tatsukawa: J. Phys. Soc. Jpn. 47 (1979) 1739.
11) C. Kittel:Phys. Rev. 71 (1947) 270; Phys. Rev. 73 (1948) 155.
12) C. W. Haas and H. B. Callen: Magnetism, ed. G. T. Rado and H. Suhl (Academic, 1963) Vol. 1, p. 449.
13) M. Date, K. Okuda and K. Kadowaki: J. Phys. Soc. Jpn. 42 (1977) 1555.
14) T. Nagamiya: Prog. Theor. Phys. 6 (1951) 350.
15) F. Keffer and C. Kittel: Phys. Rev. 85 (1952) 329.
16) F. M. Johnson and A. H. Nethercot, Jr.: Phys. Rev. 114 (1959) 705.
17) K.L.I. Kobayashi, Y. Kato, Y. Katayama and K. F. Komatsubara: Solid State Commun. 17 (1975) 875.

APPENDIX

Ferromagnetic Resonance

1) Resonance condition

According to Kittel,[11] the resonance frequency for an ellipsoidal sample possessing a magnetic anisotropy with the static magnetic field parallel to one of the principal axes of the ellipsoid which is also the preferred crystallographic axis for easy magnetization is given by

$$\omega = g\frac{e}{2mc}\left\{[H_z + (N_x-N_z)M_s + 2\frac{K_o}{M_s} + \alpha\frac{K_1}{M_s}]\times[H_z + (N_y-N_z)M_s + 2\frac{K_o}{M_s} + \alpha\frac{K_1}{M_s}]\right\}^{1/2}, \qquad (A1)$$

where g is the g-factor; $\omega/2\pi$ the microwave frequency; H_z the applied magnetic field; K_o the uniaxial term, K_1 the cubic term of the anisotropy; M_s the saturation magnetization; N_x, N_y and N_z the demagnetization constants; and α=2 or -1/4 depending on whether the <100> or <111> direction is the easy axis. As usual, e is the electronic charge, m is the electronic mass and c is the speed of light. For an arbitrarily shaped sample, the resonance condition is very complicated. For a spherical sample, $N_x=N_y=N_z$, and Eq. (A1) reduces to

$$\omega = g\frac{e}{2mc}[H_z + 2K_o/M_s + \alpha K_1/M_s]. \qquad (A2)$$

2) Linewidth

Line broadening is by (a) porosity due to the random demagnetization fields caused by voids and defects in single or polycrystals, and (b) the random anisotropy fields due to the random orientation of the crystallites in a polycrystal. Resonance linewidths of polycrystalline samples are generally one or two orders of magnitude larger than those of the single crystal samples of the same material. Therefore unlike paramagnetic resonance, ferromagnetic resonance cannot possibly be done in powdered samples. Preferably it has to be performed on polycrystals, but best on single crystals. The study of the variation of linewidths with temperature gives us information about the nature of magnon scattering processes as well as the nature of magnetic transitions.

3) Resonance frequency shifts

Resonance frequency shifts can be due to several factors viz. (a) shifts as a function of the amplitude of microwave field applied, and (b) as a function of temperature. Study of these effects would give us information about spin waves and magnon scattering processes as well as the nature of magnetic transitions.

Antiferromagnetic Resonance

1) Resonance condition

The resonance condition can be explained by the following equation derived by Nagamiya, Keffer and Kittel,[14,15]

$$\omega = g\frac{e}{2mc}\left[(2H_E H_A)^{1/2} \pm H_o(1 - \alpha/2)\right] \quad , \qquad \text{(A3)}$$

where g is the g-factor; $\omega/2\pi$ the microwave frequency; α the ratio of the parallel and perpendicular susceptibilities; H_E the Weiss exchange field; H_A the anisotropy field; and H_o the applied static magnetic field. As before, e is the electronic charge, m is the electronic mass and c is the speed of light. The above equation is applicable to crystals possessing tetragonal symmetry. For cases involving cubic symmetry, the term, $(1 - \alpha/2)$, becomes unity. Normally, antiferromagnetic resonance is performed on single crystals.

2) Temperature dependence of linewidths

This can be explained by the simplified thermal fluctuation model developed by Townes (see Ref. 16) given by the equation below,

$$\Delta H = \frac{2H_A(0)}{n}\left[\frac{1}{B_S(T/T_N)} - B_S(T/T_N)\right], \qquad \text{(A4)}$$

where ΔH is the linewidth; $H_A(0)$ the anisotropy field at 0 K; B_S the Brillouin function for spin S; and n the number of neighbours with aligned spin direction. At T_N, the Neel temperature, the linewidths tend to diverge to infinity. At temperatures above or below T_N, the linewidths decrease with increasing or decreasing temperature respectively.

3) Temperature dependence of resonance condition

Below T_N, H_o for resonance decreases (high-temperature mode) or increases (low-temperature mode) for a fixed microwave frequency as the temperature decreases. Above T_N, H_o for resonance for a fixed microwave frequency is constant since this is in the paramagnetic region. For a cubic crystal, the resonance condition is for a high-temperature mode,

$$H_o = \omega\frac{2mc}{ge} - (2H_E H_A)^{1/2} , \qquad (A5)$$

or for a low-temperature mode,

$$H_o = (2H_E H_A)^{1/2} - \omega\frac{2mc}{ge} . \qquad (A6)$$

The quantity, $(2H_E H_A)$, is temperature-dependent.